Tensile and Fatigue Behavior of Aluminum Oxide Fiber Reinforced Magnesium Composites: Part I. Fiber Fraction and Orientation

J. E. HACK, R. A. PAGE, and G. R. LEVERANT

The mechanical behavior of commercially pure magnesium reinforced with FP aluminum oxide fibers has been studied as a function of fiber fraction and orientation. Test specimens included material of two different volume fractions of fiber and four different fiber orientations. Axial properties were dependent on the fiber content and generally followed the rule of mixtures. Of the off-axis properties, only the elastic modulus exhibited a significant dependence on fiber content. Off-axis loading resulted in large reductions in both the tensile and fatigue properties. The reductions coincided with a change in fracture morphology from fracture across fibers during axial loading to fracture along the fiber direction for off-axis loading. A weak fiber/matrix interface was found to be responsible for the drop in tensile properties, and a combination of a weak matrix and a weak fiber/matrix interface were responsible for the reduced fatigue resistance.

I. INTRODUCTION

THE reinforcement of metal matrices with high strength and high modulus synthetic fibers to produce a hybrid material possessing attractive structural properties is not a new concept. The combination of recently developed high strength and modulus ceramic fibers with lightweight, ductile metal matrices (principally magnesium and aluminum) has spurred renewed interest in the potential of these materials for applications requiring high specific strength and stiffness, toughness, and fatigue resistance. Implementation of advanced metal matrix composite materials in structural applications has always suffered, however, due to a lack of a quantitative relationship between microstructure and mechanical behavior.

Although a great deal of work has been performed on fracture mechanisms in metal matrix composites,[1-4] the results to date have been quite contradictory in nature. The inconsistencies arise from the complex interaction of the fiber/matrix interfacial region with various applied states of stress. In addition, the presence of the fiber/matrix interface in these composites introduces several mechanisms of crack propagation in addition to those observed in monolithic materials.[5] Also, standard metallurgical techniques for modifying the properties of the matrix material (*i.e.*, alloying, heat treatment, deformation processing, *etc.*) affect the metallurgical structure and properties of the interfacial region as well.[6,7] Thus, the effects of processing variables on composite behavior through microstructural changes in the matrix are difficult to separate from the effects of those variables on the fiber/matrix interface.

A research program was initiated to overcome these difficulties by developing quantitative relationships between matrix microstructure, composition and properties, fiber orientation and volume percent, and fatigue crack growth behavior in these materials through direct observations of the effects of these variables on the strain field at the tip of a growing crack. The program is aimed at determining the local sequence of events at the tip of a fatigue crack (*i.e.*, matrix failure *vs* fiber failure *vs* interfacial decohesion) and the critical strain accumulation required for these events to occur. However, very little data exist on the relationships between microstructure and crack growth resistance in metal matrix composites. Hence, the initial phase of the overall program was designed to characterize the tensile and fatigue behavior of a model material. The results of that characterization will be presented in this paper while the crack tip strain characterizations will be reported at a later date.

J. E. HACK and R. A. PAGE, Senior Research Metallurgists, and G. R. LEVERANT, Assistant Director, are with the Department of Materials Sciences, Southwest Research Institute, 6220 Culebra Road, San Antonio, TX 78284.

Manuscript submitted September 8, 1983.

II. EXPERIMENTAL

The model material chosen for this study was commercially pure magnesium reinforced with Al_2O_3 fibers.* This material was selected for its microstructural simplicity and, more importantly, batch-to-batch reproducibility. Two lots of material which varied only in the amount of fiber present, 35 vol pct *vs* 55 vol pct, were employed. In both, continuous Al_2O_3 fibers of 20 μm average diameter were laid up in a unidirectional manner. A metallographic section through one of the composite plates is shown in Figure 1. The presence of extremely large grains, some of which extend over nearly the entire thickness, is evident. The large grains of Figure 1 are typical of both the 35 and 55 vol pct materials.

*The composite plates were manufactured by E. I. DuPont de Nemours and Co. by liquid infiltration of FP Al_2O_3 fibers.

The specimens utilized for both the tensile and fatigue tests were 15.2 cm long with 1.27 cm × 0.25 cm rectangular cross sections. Machining was performed with the Al_2O_3 fibers lying parallel to the 15.2 cm × 0.25 cm face and oriented at 0, 22.5, 45, and 90 deg to the 15.2 cm × 1.27 cm face and the tensile axis. Aluminum tabs were bonded to both ends of the specimens for gripping purposes. Strain gages, aligned to measure tensile strains, were attached on opposite faces of the tensile specimens.

The tensile and fatigue tests were both carried out at room temperature in a closed-loop hydraulic testing system. The tensile tests, which yielded information on the effect of fiber

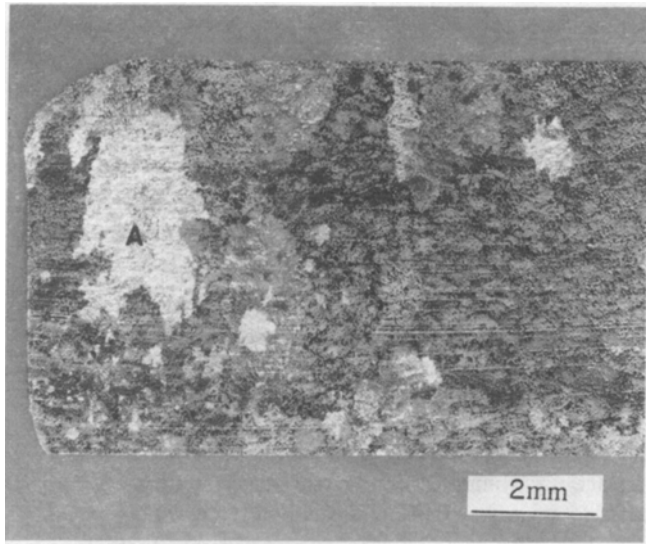

Fig. 1 — Polished and etched transverse section of 35 vol pct Al_2O_3 fiber reinforced CP Mg. Note large grains present as in Area A.

volume fraction and fiber orientation on the elastic modulus (E), yield strength (YS), ultimate tensile strength (UTS), and elongation (e) were performed under displacement control at a strain rate of 8.3×10^{-5} per second. Both strain, determined from the strain gages, and load were monitored continuously during testing. Comparison of strain readings from the front and back gages indicated that bending was not significant in these tests. The fatigue tests were run under load control at a frequency of 10 Hz and an R-ratio of 0.1. The number of cycles to failure was determined as a function of maximum stress, fiber volume fraction, and fiber orientation. Tests which did not result in failure in 1 to 2×10^6 cycles were terminated.

III. RESULTS

A. *Tensile Behavior*

The results of the tensile tests, *i.e.*, the YS, UTS, E, and e, are presented in Table I. It is apparent from these data that fiber orientation affected all four tensile parameters. The most dramatic effect was found in the YS where a 22.5 deg misorientation of the fibers decreased the YS by about an order of magnitude. The UTS was also a strong function of fiber orientation, as is evident from Figure 2. In fact, at 90 deg the YS and UTS had dropped to a value approximately equal to those of sand-cast CP magnesium (21 and 90 MPa, respectively).[8] The elongation showed an abrupt increase as the fiber orientation went from 0 deg to 22.5 deg, then dropped off with increasing angle for both volume fractions. The ductility in the 55 vol pct material tended to be slightly higher at intermediate angles. The elastic modulus was the least sensitive to fiber orientation, exhibiting a factor of two difference between the axial and transverse moduli. The data further indicate that the elastic modulus at all orientations and the axial YS and UTS were increased by increasing the fiber volume fraction. The YS and UTS of off-axis specimens, however, were not sensitive to the fiber volume fraction to any significant degree. The convergence of the UTS curves for 35 and 55 vol pct material at 22.5 deg and beyond in Figure 2 further illustrates the negligible effect that fiber content has on off-axis strength.

Table I. Tensile Properties of 35 and 55 Vol Pct Al_2O_3 Fiber Reinforced CP Magnesium

Vol Pct Al_2O_3	Orientation, Deg.	YS, MPa	UTS, MPa	E, GPa	e_f, Pct
35	0 (axial)	213	383 (396)	149 (162)	0.26
35	22.5	34	207	116	0.52
35	45	23	108	90	0.45
35	90 (transverse)	21	104	85	0.42
55	0 (axial)	321*	567* (571)	197 (229)	0.30*
55	22.5	27	196	155	0.81
55	45	30	157	124	0.58
55	90 (transverse)	18	67	90	0.24

All values are the averages of duplicate tests except where noted. Values in parentheses are calculated from the rule-of-mixtures (ROM).

*Values from a single test. Second specimen failed at 400 MPa due to the presence of a large process defect.

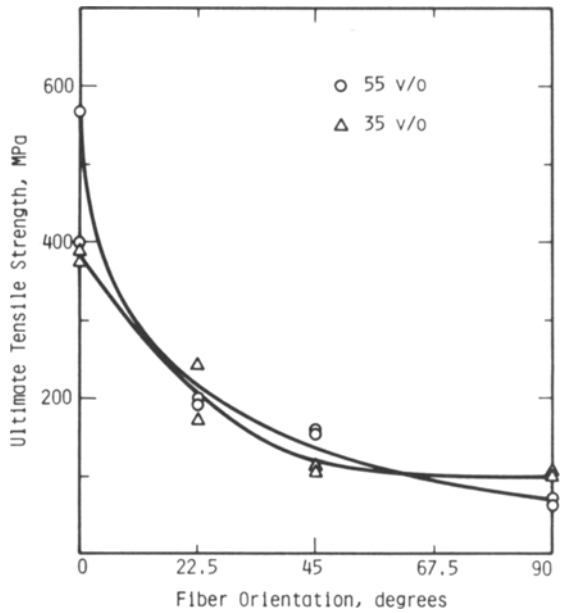

Fig. 2 — Effect of fiber orientation on ultimate tensile strength for both 35 and 55 vol pct Al_2O_3 fiber reinforced CP Mg.

Fractographic characterization of the tensile specimens indicated that failure of the axial specimens occurred at 90 deg to the applied stress, *i.e.*, through the fibers. The role that defects can play in the tensile failure of axial specimens is illustrated by the wide scatter in the axial 55 vol pct data. Sample 55-0-A which had a UTS 30 pct lower than Sample 55-0-B, failed at a massive process defect, roughly 2500×200 μm. Although Samples 55-0-B, 35-0-A, and 35-0-B contained similar defects on the order of ten times the fiber diameter (20 μm), the UTS was in line with previously published values. This implies that defects have to cover a significant fraction of the specimen cross section to affect tensile properties. The nature of the defects will be discussed in detail in the next section on fatigue behavior.

Failure of all the off-axis 55 vol pct samples and the 35 vol pct samples tested at 45 and 90 deg occurred along the fiber axis by decohesion of the fiber/matrix interface.

Failure of the 35 vol pct samples tested at 22.5 deg occurred at an angle close to 90 deg by a mixture of interfacial decohesion and fiber cracking. No evidence of initiation at process defects was found in any of the off-axis tensile specimens.

B. *Fatigue Behavior*

The fatigue resistance of both 35 and 55 vol pct materials was found to be a function of the fiber orientation. Increasing the angle between the fiber axis and the stress axis resulted in a reduction in the fatigue resistance, as evidenced by the compendium of S-N curves in Figure 3. (The solid and dashed lines in the figure represent a least squares fit to the data. The arrowed data represent samples which had not failed by $\sim 10^6$ cycles and were thus terminated.) As observed in the tensile behavior, the higher volume fraction of fibers resulted in a dramatic increase in the fatigue resistance of the axial specimens. The close grouping of the off-axis data, however, indicates that fiber content did not strongly influence off-axis fatigue strength. The data presented in Figure 3 also indicate that fatigue resistance scales roughly with the *UTS*. This is more obvious in Figure 4 in which all of the fatigue data, 35 and 55 vol pct and axial through transverse geometries, has been normalized with respect to the appropriate *UTS*. The normalized data all lie within a band which yields an endurance limit, defined as the stress which results in failure in 10^6 cycles, of between 0.6 and 0.95 times the *UTS* with an average value of about 0.75 times the *UTS*.

The fatigue and overload regions of axial fatigue specimens both exhibited fractographic features similar to those of the axial tensile specimens. In both cases cracking occurred across the fibers at roughly 90 deg to the tensile axis. The features of the fatigue and overload failures were so similar that it was impossible to determine the extent of fatigue cracking from examinations of the fracture surface. River markings on the fracture surfaces did, however, indicate that cracking had initiated at process defects. Two distinct types of defects were found to be responsible for

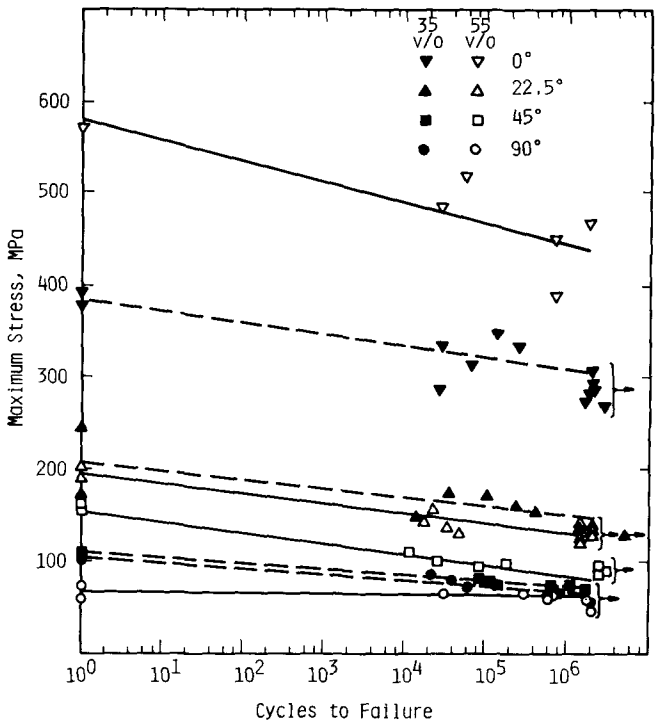

Fig. 3—Combined S-N curves for both 35 and 55 vol pct Al_2O_3 fiber reinforced CP Mg illustrating the effect of fiber volume fraction as a function of orientation.

fatigue crack initiation: (1) individual fibers which had broken and fallen perpendicular to the stress axis during processing, and (2) large clumps of Al_2O_3 grains which were an order of magnitude larger than the average fiber diameter. Failure of both of these defects was determined (Part II) to be due to delamination of the Al_2O_3/Mg interface. Examples of the two types of defect are shown in Figure 5.

In contrast to the axial specimens, off-axis specimens failed generally parallel to the fiber axis. Furthermore, a striking difference was observed between the fracture morphology of the fatigue and overload regions of the off-axis

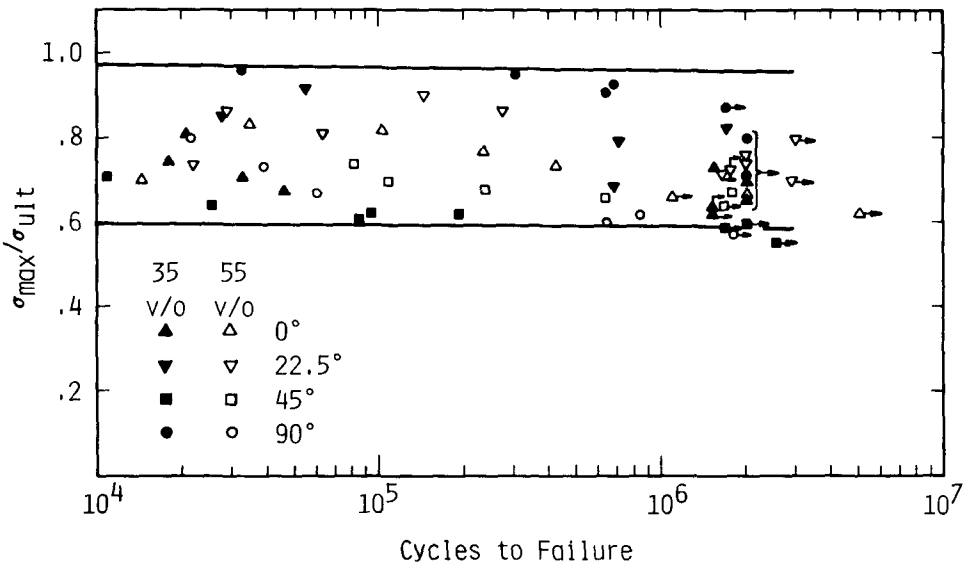

Fig. 4—Fatigue data for both 35 and 55 vol pct Al_2O_3 fiber reinforced CP Mg normalized with respect to the *UTS*.

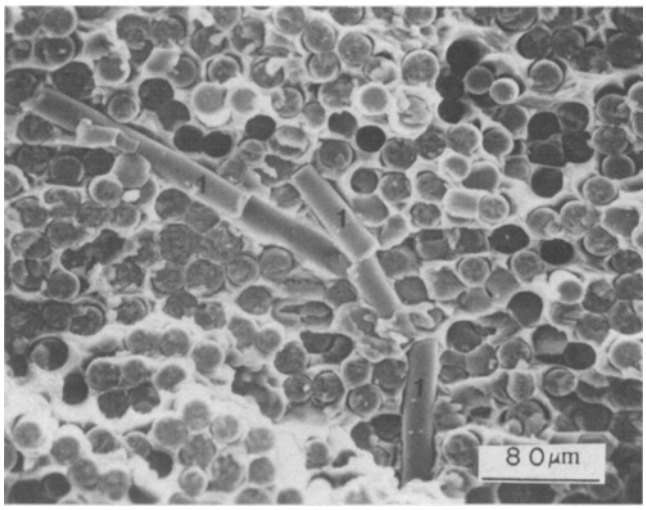

(*a*)

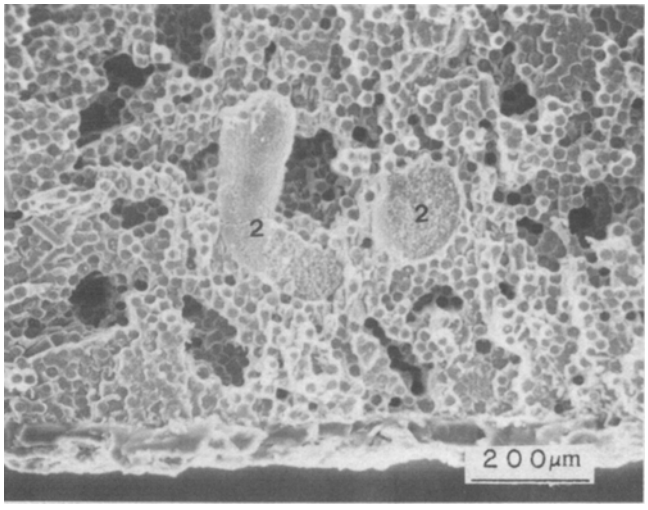

(*b*)

Fig. 5 — Typical process defects responsible for crack initiation in axial specimens: Al_2O_3 fiber reinforced CP Mg (*a*) transverse fibers (Area 1), and (*b*) clumps of Al_2O_3 grains (Area 2).

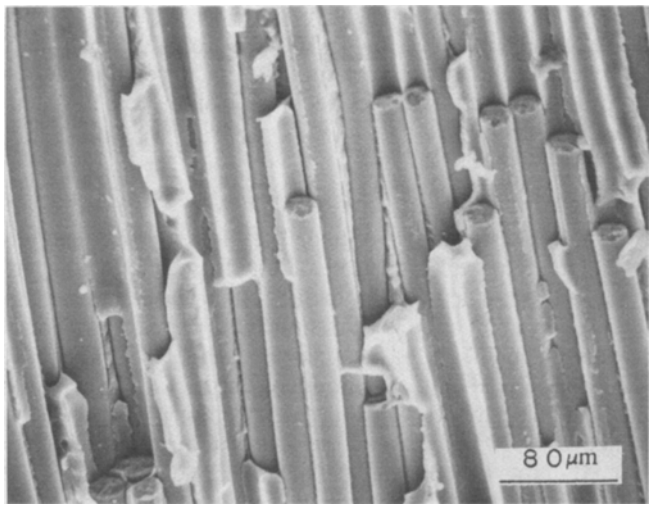

(*a*)

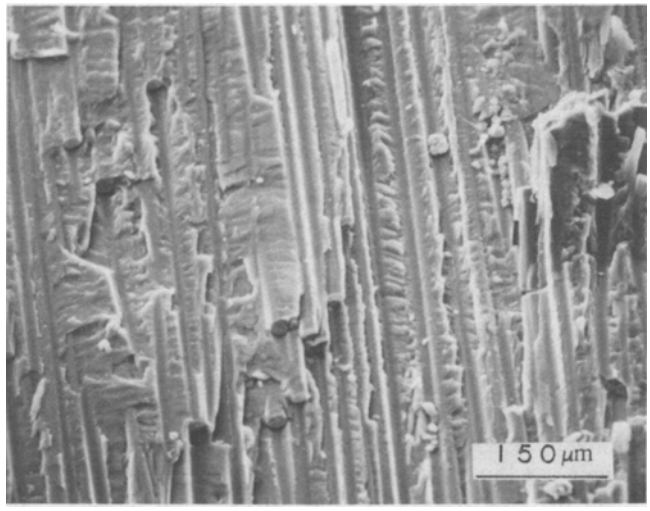

(*b*)

Fig. 6 — Scanning electron micrographs of typical overload (*a*) and fatigue (*b*) failures in off-axis specimens of Al_2O_3 fiber reinforced CP Mg. Note that the failure in overload occurs almost exclusively along fiber/matrix interfaces while subcritical fatigue crack growth occurs parallel to the interfaces but primarily through the matrix.

specimens. This difference is illustrated by the fractographs of Figure 6. The overload regions exhibited features identical to those of the off-axis tensile failures, as would be expected. Delamination of the fiber/matrix interface was the primary mode of failure in all but the 35 vol pct material oriented at 22.5 deg. Thus, the fracture was oriented along the fiber axis in all but the 35 vol pct material oriented at 22.5 deg. The overload failure mode was mixed in these samples, consisting of roughly equal amounts of interfacial delamination and flat fracture across fibers, and occurred approximately perpendicular to the tensile axis.

Fatigue cracking in all of the off-axis specimens occurred along the direction of the fiber axis by a combination of delamination of the fiber/matrix interface and cracking of the magnesium matrix. Of these, matrix cracking, which exhibited a brittle, crystallographic morphology reminiscent of cyclic cleavage,[9] as in Figure 7, was the predominant mode. In many instances the crystallographic features were maintained over distances corresponding to from tens to hundreds of fiber diameters. Figure 8 is typical of one such area. Examination of the fatigue regions did not indicate that process defects acted as initiation sites as they had in the axial tests. Metallographic sections taken through a number of the fatigue regions revealed numerous secondary cracks, many of which were entirely situated in matrix material. An example of the secondary cracking observed is presented in Figure 9.

C. *Fiber Spacing*

Average fiber spacings were determined from fatigue and overload regions of both 35 and 55 vol pct material by counting the number of fibers intersected by lines of known length passed randomly in the fracture plane and perpendicular to the fiber axis. For comparison purposes, average

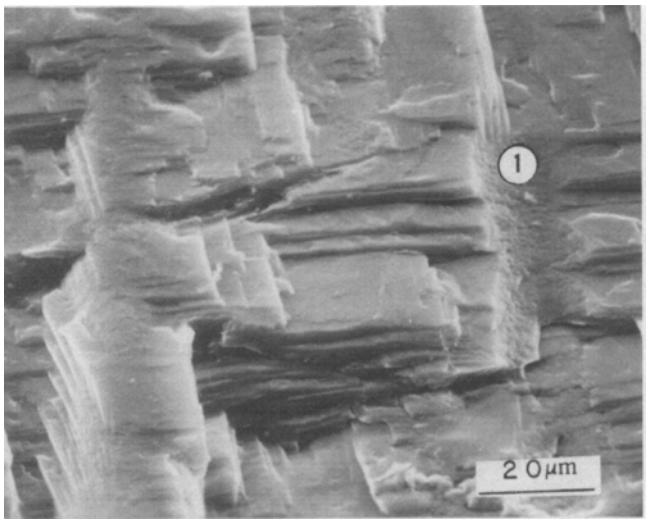

Fig. 7—High magnification view of typical cleavage-like matrix fracture morphology in fatigue thumbnail regions of off-axis specimens of Al_2O_3 fiber reinforced CP Mg. Fiber trough is visible in region 1.

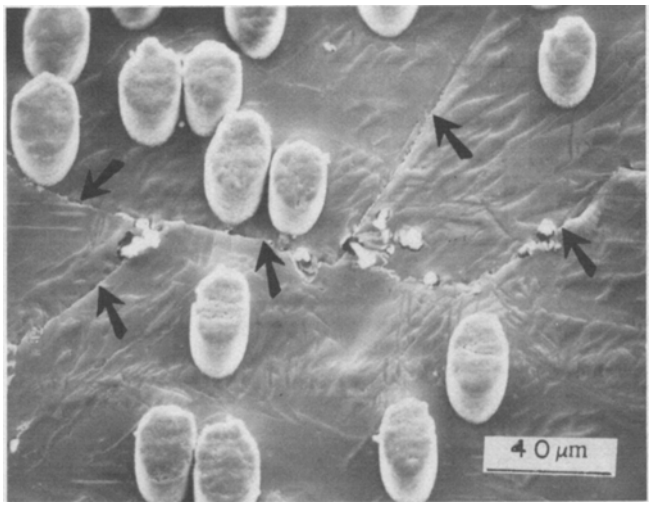

Fig. 9—Scanning electron micrograph of a typical secondary crack located in the matrix of an off-axis fatigue specimen of Al_2O_3 fiber reinforced CP Mg. Note that the cracking avoids fiber/matrix interfaces during subcritical crack growth (crack path denoted by arrows).

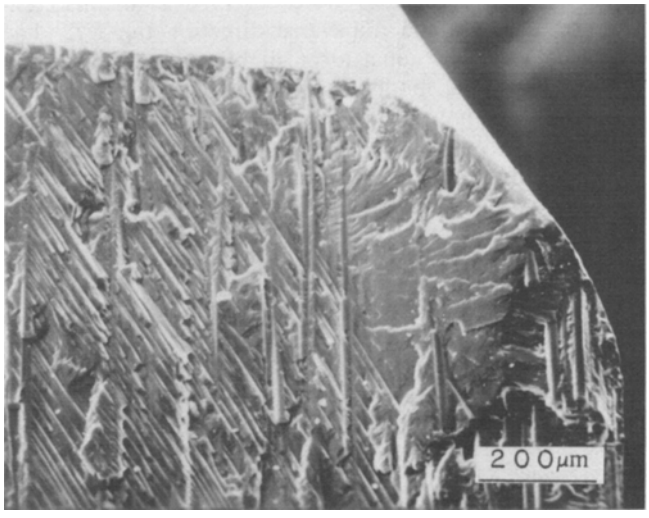

Fig. 8—Scanning electron micrograph of typical off-axis fatigue region illustrating the large distances over which crystallographic features extend.

Table II. Fiber Spacing Comparison in Fatigue and Overload Failure

Vol Pct Fiber	Orientation	Location	Average Spacing, μm
35	—	transverse section	44
35	—	transverse section	37
35	45 deg	fatigue region	74
35	45 deg	fatigue region	197
35	45 deg	overload region	23
35	90 deg	fatigue region	74
35	90 deg	fatigue region	60
35	90 deg	fatigue region	75
35	90 deg	overload region	24
55	—	transverse section	29
55	—	transverse section	30
55	22.5 deg	fatigue region	43
55	22.5 deg	overload region	24
55	45 deg	fatigue region	46
55	45 deg	overload region	20
55	90 deg	fatigue region	35
55	90 deg	overload region	21

spacings were also determined on metallographic sections cut transverse to the fiber axis. In this case the lines were passed randomly in a plane perpendicular to the fiber axis. The data, which represent averages obtained from 3 to 10 separate counts, are presented in Table II. Spacings obtained from fatigue regions were consistently larger than those obtained from random transverse sections. On the other hand, spacings obtained from the overload regions were consistently smaller than those obtained from random transverse sections.

D. *Auger Spectroscopy*

A number of transverse specimens were fractured *in situ* in a Physical Electronics 595 scanning Auger microprobe. The *in situ* fracture occurred along fiber/matrix interfaces (Figure 10) in a manner similar to the off-axis tensile and overload failures. Spectra taken from the fiber trough and the fiber surface are presented in Figures 11(a) and (b), respectively, Comparison of the fine structure of the magnesium peaks and the ratio of the oxygen to magnesium peak heights with spectra taken from laboratory standards[10] indicates that the trough side of the fracture was metallic magnesium with a small amount of oxygen and the fiber side of the fracture was an oxide of magnesium, most likely MgO. Aluminum was not detected on either the trough or the fiber surface.

IV. DISCUSSION

As mentioned in the introduction, Al_2O_3 fiber reinforced magnesium was chosen for this investigation because it was representative of the most recent generation of composite materials which contain high performance, state-of-the-art

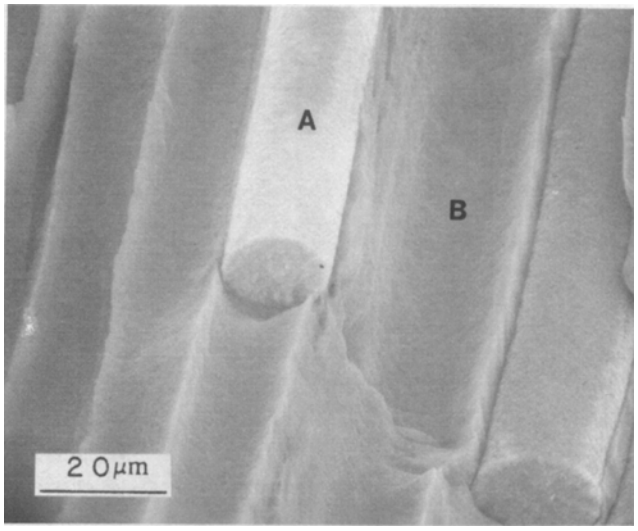

Fig. 10 — Scanning electron micrograph of the failure obtained in the scanning Auger microprobe. Typical exposed fiber in Area A, fiber trough in Area B.

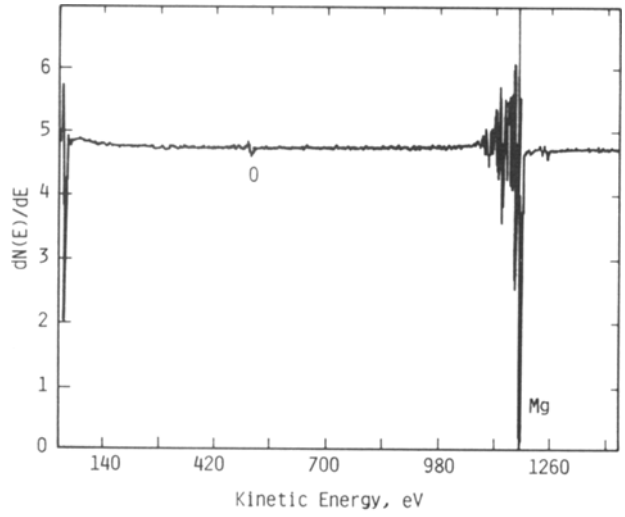

Fig. 11 — Auger electron spectra taken from the fiber trough (*a*) and the fiber surface (*b*) of an *in situ* fractured specimen.

fibers in a ductile metal matrix. The test results obtained for the Al_2O_3 fiber reinforced commercially pure magnesium indicate the effect of fiber orientation and volume fraction on tensile and fatigue properties and provide a basis from which the effects of changes in various material parameters such as matrix alloying and fiber/matrix interfacial strength can be evaluated.

A. *Tensile Behavior*

The tensile results indicate that Al_2O_3 fiber reinforced magnesium tested in the axial direction responds to changes in fiber content in much the same manner as other composites which have been investigated,[11,12,13] *i.e.*, *YS*, *UTS*, and *E* increase with increased fiber content. This behavior is consistent with the trend predicted by the rule of mixtures (ROM). Although the ROM values for *UTS* were quite close to those observed for axial specimens, *E* was overestimated by approximately ten percent for both 35 and 55 vol pct materials. The ROM calculations were made with *UTS* Mg = 90 MPa;[14] *UTS* Al_2O_3 = 965 MPa;[15] *E* Mg = 45 GPa;[14] *E* Al_2O_3 = 384 GPa.[15]

The off-axis results illustrate the dramatic effect that fiber orientation can have in composites of this type. Large drops in *YS*, *UTS*, and *E* were observed at all misorientations tested. In the transverse direction the *UTS* had dropped to a value equal to or slightly below that of the matrix alone. The modulus, however, was approximately doubled by the presence of the fibers. The sharp reduction in *UTS* and *YS* was related to a change in failure mode from flat fracture across fibers to delamination of the fiber/matrix interface.

Resolution of the stresses into the fiber axis, interface normal, and interface shear components yields:[16]

$$\sigma_{11} = \sigma_A \cos^2 \Theta \quad [1]$$

$$\sigma_{22} = \sigma_A \sin^2 \Theta \quad [2]$$

$$\sigma_{12} = \frac{\sigma_A}{2} \sin^2 \Theta \quad [3]$$

respectively, where σ_A is the applied stress. A plot of normalized stress *vs* angle is given in Figure 12.

If the interfacial strength was a significant fraction of the fiber strength, the composite tensile strength would be expected to increase with misorientation angle. Interfacial

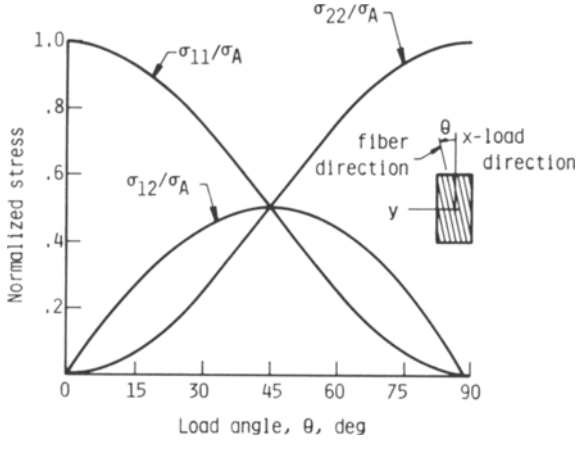

Fig. 12 — Variation of material axes stress in unidirectional composite plotted against load direction (Ref. 16).

shear controlled failure would cause the *UTS* to fall with increasing Θ up to 45 deg and then rise as Θ increased to 90 deg. If the off-axis failure occurred due to normal stresses, however, the *UTS* would be expected to show a constant decrease with increasing Θ. The lack of shearing in the troughs of failed off-axis specimens and the tensile behavior shown in Figure 2 strongly support the ideas that the interface is very weak with respect to normal forces. Even at 22.5 deg where σ_{11}/σ_A and σ_{22}/σ_A are 0.85 and 0.15, respectively, the weakness of the interface in comparison with the axial composite strength is dramatic enough to induce predominantly interfacial failure. An independent analysis based on stress intensity factors also clearly shows the important role of the normal stress.[17]

A similar analysis for strains can be used to explain the elongation behavior. Since macroscopic deformation is restricted to occur parallel to the fiber orientation in off-axis specimens, the shear strain would be expected to control the ductility of the composite. As can be seen from Figure 13,[16] the interfacial shear strains in a unidirectional composite increase abruptly with Θ as the angle of misorientation increases from 0 deg and then falls off slowly with increasing Θ. This is precisely the behavior in *e* observed in Table I.

The Auger results indicate that off-axis failure occurs along a magnesium/magnesium oxide interface, which must be concluded to be the matrix/reaction zone interface. Formation of magnesium oxide in the reaction zone is predicted by thermodynamic considerations, as is the formation of $MgAl_2O_4$ spinel. Levi *et al.*[18] have shown that MgO can form when the magnesium content of the matrix is high. Thus, it can be concluded that a reaction zone of MgO formed during casting and that the interface between the reaction zone and the matrix was the site of off-axis failure. The nature of the interface region is discussed in Part II of this pair of papers.

The insensitivity of the off-axis *YS* and *UTS* to changes in fiber content is also noteworthy. Similar behavior has been observed when matrix failure predominates.[13] On the other hand, a strong dependence on fiber content has been observed when failure occurs by fiber splitting.[11] These observations suggest that, unless the fibers participate in off-axis failure, the off-axis *YS* and *UTS* do not benefit greatly from increases in the fiber volume fraction. Large benefits would be expected, however, from increases in the fiber/matrix interface strength. This has been observed with an alloyed Mg matrix reinforced with Al_2O_3 and is reported in Part II.

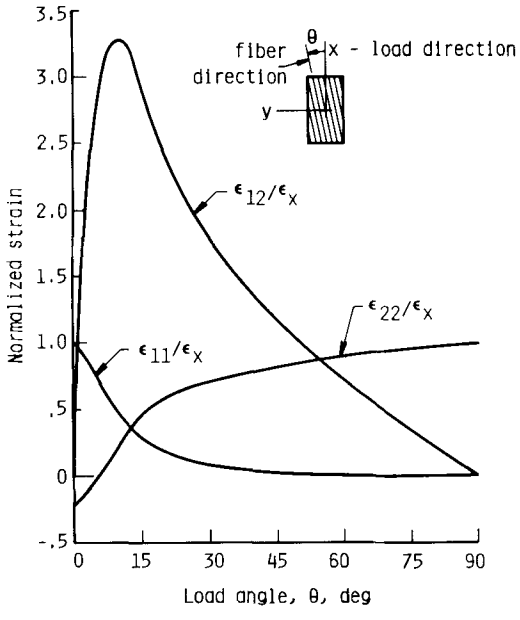

Fig. 13 — Variation of material axes strains in a typical unidirectional composite plotted against load direction (Ref. 16).

B. *Fatigue Behavior*

The fatigue resistance of the Al_2O_3 fiber reinforced magnesium, as measured by S-N curves, mirrored the *UTS*. Hence, all of the correlations that were made between fiber content or orientation and tensile strength also apply to the fatigue life behavior. Increases in fiber content would therefore be expected to increase lifetimes in axial fatigue but provide little or no benefit for off-axis loadings, as was observed. Similarly, increases in misorientation angle were found to sharply depress the S-N curves.

One of the most interesting aspects of this study was the off-axis subcritical fatigue crack growth behavior. Although the fiber/matrix interface was weak, as demonstrated by the off-axis tensile and overload failures, fatigue cracking occurred primarily through the magnesium matrix.* The matrix cracking, which was brittle and crystallographic in appearance, may be similar to the crystallographic Stage I cracking which has been observed along slip planes and twin boundaries in monolithic magnesium.[19] The major role of the fibers in fatigue is believed to be one of channeling the fatigue cracks in a direction parallel to the fiber axis, although interfacial delamination did play at least a minor role in the cracking.

All the off-axis tensile data indicate that the interface between the fiber and matrix is extremely weak. Since fatigue cracks appear to have initiated in the matrix and showed only a transition to interfacial failure at overload, it is safe to assume that initiation occurred early in the lifetime. Thus, the lifetime of the off-axis specimens was propagation controlled even in the high cycle regime. From the geometry of the thumbnails, it is known that the stress intensity did not exceed approximately 7 MPa · $\sqrt{m}$ during the off-axis fatigue tests.[17] Crack growth rates in monolithic Mg alloys have been found to be on the order of 10^{-7} m/cycles at these levels of stress intensity.[20] Similar behavior has been found in directionally-solidified nickel base superalloys[21] and other metal-matrix composite systems[22] where initiation occurs early in life but fatigue crack growth rates at the critical stress intensity are still close to the near-threshold regime.

The implications of these results are twofold. First, fiber/matrix interface strength should play a primary role in the off-axis S-N behavior through its control of overload resistance but only a secondary role in the off-axis fatigue crack propagation behavior since the primary fracture morphology was not interface related. Second, matrix strength should play a primary role in both off-axis S-N behavior and

*The observation that fatigue cracking occurred primarily through the matrix is supported by the fractography, Figures 9 and 11, the larger than average fiber spacing observed on the fracture surfaces, Table II, and the observations of the secondary cracks situated entirely in the matrix, Figure 12. Furthermore, sections through the thumbnails indicated that the fatigue cracks tended to step around fibers.

fatigue crack propagation since it controls the primary fracture morphology. Alloying of the matrix therefore appears to be the most promising approach to improved off-axis properties since, through proper alloy additions, it may be possible to increase both matrix and interfacial strengths.

C. *Process Defects*

The fractographic results on the axial tensile and fatigue specimens indicated that process defects play a role in crack initiation at 0 deg. In fact, fatigue crack initiation could always be traced to a process defect. However, the *UTS* of the composite only deviated from the rule of mixtures when an unusually large defect was present (Figure 3). Defects of this size were not found in any other specimen. Although fatigue crack initiation most likely occurred early in the specimen lifetime due to the presence of the process defects, the endurance limit in the axial fatigue specimens remained at approximately 70 pct of the ROM *UTS* value. This was the same range as was found for the off-axis specimens where process defects did not contribute to crack initiation. In addition, most component design considerations incorporate cross-plied fibers to offset the inferior off-axis tensile strength with respect to the axial orientation, thus providing paths for crystallographic crack initiation in the matrix. With all of these facts taken into account, it seems that, with the exception of gross defects such as that found in the 55 vol pct axial tensile specimen, the improvement in mechanical properties to be gained by the removal of the process defects would not be worth the considerable cost and effort required. Some form of non-destructive evaluation to detect gross defects is required, however.

V. CONCLUSIONS

The following conclusions can be drawn from the results obtained in the present investigation:

1. Process defects in the form of large clumps of Al_2O_3 grains and fibers which were broken and lying on their sides were preferential sites for crack initiation for both monotonic and cyclic loading along the fiber axis. However, the presence of the defects was not particularly damaging to axial tensile or fatigue properties unless the size of the defect was a significant fraction of the specimen cross section. Process defects did not play a role in crack initiation during off-axis loading.
2. Changes in the fiber content can be used to alter the axial properties. With respect to the off-axis properties, however, only the modulus is significantly affected by fiber content.
3. The weak fiber/matrix interface causes a large reduction in tensile properties when loading is off-axis. The reduction in properties is related to a change in the mode of fracture from flat fracture across fibers in the axial condition to failure along the fiber/matrix interface in the off-axis condition. An increase in interfacial strength brought about either through process modification or through alloying should yield improved off-axis properties.
4. Interfacial delamination, which was the predominant failure mode in all off-axis overload failures, occurred along the interface between the magnesium matrix and the magnesium oxide reaction zone.
5. Fatigue crack initiation and propagation during off-axis loading occurs primarily through the magnesium matrix. Hence, alloy additions designed to increase the strengths of the matrix and the fiber/matrix interface should be effective in increasing the off-axis fatigue resistance of the composite.

ACKNOWLEDGMENTS

The authors are grateful for the support of this work by the Army Research Office under Contract No. DAAG29-81-K-0049. We would also like to thank Dr. R. Sherman for performing the Auger analyses. The technical assistance of Messrs. V. D. Aaron and H. Saldana in specimen preparation and testing is also greatly appreciated.

REFERENCES

1. G. A. Cooper and A. Kelly: *J. Mech. Phys. of Solids*, 1967, vol. 15, p. 279.
2. R. E. Cooper: *J. Mech. Phys. Solids*, 1970, vol. 18, p. 179.
3. A. Kelly: *Proc. Royal Soc. London*, 1970, vol. 319, p. 95.
4. D. L. McDanels, R. W. Jech, and J. M. Weeton: *Trans. TMS-AIME*, 1965, vol. 233, p. 636.
5. A. S. Tetelman: *Composite Materials: Testing and Design*, ASTM STP 460, American Society for Testing and Materials, Philadelphia, PA, 1969, p. 473.
6. J. R. Hancock: *Composite Materials: Testing and Design (Second Conference)*, ASTM STP 497, American Society for Testing and Materials, Philadelphia, PA, 1972, p. 483.
7. G. D. Swanson and J. R. Hancock: *Composite Materials: Testing and Design (Second Conference)*, ASTM STP 497, American Society for Testing and Materials, Philadelphia, PA, 1972, p. 469.
8. *Metals Handbook*, 9th ed., ASM, Metals Park, OH, 1979, vol. 2, p. 264.
9. M. Gell and G. R. Leverant: *Acta Metall.*, 1968, vol. 16, p. 553.
10. L. E. Davis, N. C. MacDonald, P. W. Palmberg, G. E. Riach, and R. E. Weber: *Handbook of Auger Electron Spectroscopy*, 2nd ed., Physical Electronic Industries, Eden Prairie, MN, 1976, pp. 39-41.
11. K. M. Prewo and K. G. Kreider: *Metall. Trans.*, 1972, vol. 3, p. 2201.
12. P. E. Chen and J. M. Lin: *Mat. Res. Std.*, 1969, vol. 9, no. 8, p. 29.
13. K. M. Prewo and K. G. Kreider: *J. Comp. Mat.*, 1972, vol. 6, p. 338.
14. *Metals Handbook*, 8th ed., ASM, Metals Park, OH, 1961, vol. 1.
15. R. T. Pepper and D. C. Nelson: Report No. NASA CR-167999, NASA-Lewis Research Center, Cleveland, OH, September 1982.
16. C. C. Chamis and J. H. Sinclair: Report No. NASA TN D-8215, NASA-Lewis Research Center, Cleveland, OH, April 1976.
17. K. S. Chan, J. E. Hack, and R. A. Page: *Metall. Trans. A*, 1984, vol. 15A, p. 756.
18. C. G. Levi, G. J. Abbaschian, and R. Mehrabian: *Metall. Trans. A*, 1978, vol. 9A, p. 697.
19. M. J. May and R. V. K. Honeycombe: *J. Inst. Metals*, 1963-64, vol. 92, p. 41.
20. N. M. Grinberg: *Int. J. Fatigue*, 1982, vol. 4, p. 83.
21. M. Gell and G. R. Leverant: *Trans. TMS-AIME*, 1968, vol. 242, p. 1869.
22. M. Gouda, K. M. Prewo, and A. J. McEvily: *Fatigue of Fibrous Composite Materials*, ASTM STP 723, K. N. Lauritis, ed., American Society for Testing Materials, Philadelphia, PA, 1981, pp. 101-15.